H-bond network in amino acid cocrystals with H 2O or H 2O 2. the DFT study of serine - H 2O and Serine - H 2O 2

ARTICLE *in* THE JOURNAL OF PHYSICAL CHEMISTRY A · NOVEMBER 2011

Impact Factor: 2.69 · DOI: 10.1021/jp207899z · Source: PubMed

THE JOURNAL OF PHYSICAL CHEMISTRY A

ARTICLE

pubs.acs.org/JPCA

H-Bond Network in Amino Acid Cocrystals with H_2O or H_2O_2. The DFT Study of Serine−H_2O and Serine−H_2O_2

Mikhail V. Vener,*[,†] Alexander G. Medvedev,[‡] Andrei V. Churakov,[‡] Petr V. Prikhodchenko,[‡,§] Tatiana A. Tripol'skaya,[‡] and Ovadia Lev*[,§]

[†]Department of Quantum Chemistry, Mendeleev University of Chemical Technology, Miusskaya Square 9, 125047 Moscow, Russia

[‡]Kurnakov Institute of General and Inorganic Chemistry, Russian Academy of Sciences, Leninskii prosp. 31, Moscow 119991, Russia

[§]The Casali Institute of Applied Chemistry, The Institute of Chemistry, The Hebrew University of Jerusalem, Jerusalem 91904, Israel

Supporting Information

ABSTRACT: The structure, IR spectrum, and H-bond network in the serine−H_2O and serine−H_2O_2 crystals were studied using DFT computations with periodic boundary conditions. Two different basis sets were used: the all-electron Gaussian-type orbital basis set and the plane wave basis set. Computed frequencies of the IR-active vibrations of the titled crystals are quite different in the range of 10−100 cm^{-1}. Harmonic approximation fails to reproduce IR active bands in the 2500−2800 frequency region of serine−H_2O and serine−H_2O_2. The bands around 2500 and 2700 cm^{-1} do exist in the anharmonic IR spectra and are caused by the first overtone of the OH bending vibrations of H_2O and a combination vibration of the symmetric and asymmetric bendings of H_2O_2. The quantum-topological analysis of the crystalline electron density enables us to describe quantitatively the H-bond network. It is much more complex in the title crystals than in a serine crystal. Appearance of water leads to an increase of the energy of the amino acid−amino acid interactions, up to ∼50 kJ/mol. The energy of the amino acid−water H-bonds is ∼30 kJ/mol. The H_2O/H_2O_2 substitution does not change the H-bond network; however, the energy of the amino acid−H_2O_2 contacts increases up to 60 kJ/mol. This is caused by the fact that H_2O_2 is a much better proton donor than H_2O in the title crystals.

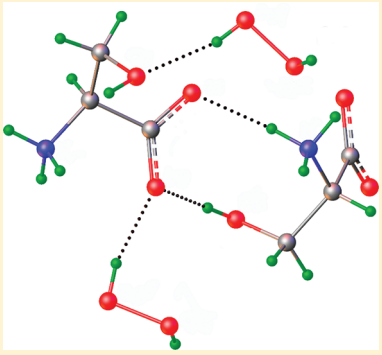

INTRODUCTION

Hydrogen bonds (H-bonds) formed by peptide−peptide and peptide−water interactions play a central role in protein folding and dynamics. The direct study of these interactions is difficult because of the complexity of the protein macromolecule.[1,2] As amino acids are the basic building blocks of proteins, it is useful to investigate the amino acid−amino acid and amino acid−water interactions that mimic some aspects of the protein structure. In the gas phase and in low-temperature inert matrices, amino acids exist in neutral form, for example, see ref 3. Interactions between amino acid neutral forms are relatively weak;[4] the energy of the O···H−N contacts is less than 25 kJ/mol.[5] The gas-phase models have limited applicability to the peptide−peptide interactions because the latter are mainly caused by the interactions between zwitterionic forms of amino acids. Adequate description of these interactions implies the explicit consideration of the intermolecular H-bond formation and, at least, the implicit consideration of environmental effects (polar solvent or crystalline environment). These effects stabilize the formation of the intermolecular $-O\cdots H-N^+$ bonds.[3,6] Theoretical studies of amino acids in water, for example, see refs 7−9, gave some valuable insight; however, they are often blurred by the spectral overlap and solvent or temperature effects. Molecular crystals present an ideal model for experimental and theoretical studies of the amino acid−amino acid and amino acid−water interactions. H-bonds in amino acid crystals were studied by IR/Raman,[10−14] tetrahertz spectroscopy,[15−18] INS,[19,20] and density functional theory (DFT) methods with periodic boundary conditions.[15,16,21] The H-bond network in these crystals is formed by the interactions between zwitterions. The energy of the intermolecular O···H−N bonds varies from 10 to 36 kJ/mol, and the shortest H···O distance is 1.73 Å.[10] The intermolecular O···H−O bonds are stronger than the O···H−N bonds, their energy vary from 24 to 39 kJ/mol, and the shortest H···O distance is 1.69 Å.[10] The H-bond network in the amino acid crystallohydrate forms is much more complex than that in amino acid crystals, due to the appearance of the amino acid−water interactions, for example, see refs 22,23. To our best knowledge, the amino acid−water interactions in crystals were not studied systematically. In fact, it is not even clear whether water is a better hydrogen donor or hydrogen acceptor in amino acid hydrates.

The interaction of natural amino acids and hydrogen peroxide is also of importance due to the ubiquity of hydrogen peroxide in biological and environmentally relevant processes.[24−26] Recently, the structures of various natural amino acid perhydrates were investigated by single-crystal X-ray diffraction.[27] Surprisingly,

Received: August 17, 2011
Revised: October 4, 2011
Published: October 17, 2011

this Article describes more crystal structures of amino acid perhydrates than the respective hydrates reported in the Cambridge Crystallographic Database (CSD, ver. 5.31, May 2010),[28] which may hint at the different propensity for hydrogen bonding with hydrogen peroxide. According to ref 27, donor hydrogen bonds formed by hydrogen peroxide in amino acid perhydrates are significantly stronger than those formed by water molecules in amino acid hydrates. Direct comparison of the hydrate and perhydrate forms of the particular amino acid gives a unique possibility to describe quantitatively the effects of isomorphism on the amino acid−amino acid, amino acid−H_2O, and amino acid−H_2O_2 interactions.

In this Article, the structure, IR spectrum, and H-bond network of serine−H_2O and serine−H_2O_2 crystals are studied by DFT methods with periodic boundary conditions. Two different basis sets are used: the all-electron Gaussian-type orbital basis set and the plane wave basis set. The aims of this Article are as follows: (1) to give a quantitative description of the H-bond network in serine−H_2O/H_2O_2 crystals using the Bader analysis of the periodical electronic density; (2) to estimate the role of anharmonicity in the mid-IR spectrum of the considered cocrystals; and (3) to compare the computed frequencies of the IR-active vibrations of the title crystals in the tetrahertz region.

COMPUTATIONAL DETAILS

DFT Calculations with Periodic Boundary Conditions. Two different codes are used in the present study: CRYSTAL06[29] and CPMD.[30] In the CRYSTAL06 calculations, different functionals (B3LYP, BLYP, and PBE) are used with all-electron Gaussian-type orbital basis sets (6-31G**, 6-311G**). The BLYP/6-311G** approximation is found to give the best results for the O−O, O···O, and O···N distances in comparison with the experimental values and is used in the present study (Tables S1 and S2). The default CRYSTAL06 options are used for the level of accuracy in evaluating the Coulomb and Hartree−Fock exchange series and a grid used in evaluating the DFT exchange-correlation contribution. Tolerance on energy controlling the self-consistent field convergence for geometry optimizations and frequencies computations is set to 1×10^{-8} and 1×10^{-10} hartree, respectively. The number of points in the numerical first derivative calculation of the analytic nuclear gradients equals 2. The shrinking factor of the reciprocal space net is set to 3. Frequencies of normal modes were calculated within the harmonic approximation by numerical differentiation of the analytical gradient of the potential energy with respect to atomic position.[31] The IR intensities for normal modes were calculated from the dipole moment derivatives determined using well-localized Wannier functions of the unit cell to calculate the Born charge tensors.[31,32] Vibrational mode descriptions were based on the consideration of deuterium-substituted species; for example, the frequency and IR intensity of the O3−H7 (Figure 1) stretching vibrations have been performed for crystals in which all H atoms belonging to the NH_3^+, CH, CH_2 groups, and H_2O/H_2O_2 species were substituted on D atoms.

The obtained geometrical parameters were used in the computation of periodical electronic wave functions by the CRYSTAL98 program[33] at the BLYP/6-311G** level of approximation. The quantum-topological analysis of the crystalline electron density was performed by the TOPOND computer program.[34] Details of the electron-density topological analysis of the molecular crystals were presented elsewhere.[35,36] The following electron-density

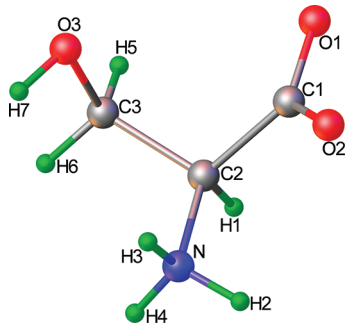

Figure 1. Atomic labeling scheme for a serine molecule in the serine−H_2O/H_2O_2 crystals.

features at the H···X (X = O, N) intermolecular bond critical point are considered: the values of (i) the electron density, ρ_b, and (ii) the potential energy density, V_b. The first value may be measured experimentally by means of the X-ray diffraction, while V_b is used to estimate the energy of the particular H-bond, E_{int}[37,38] (in atomic units):

$$E_{int} = (1/2)V_b \quad (1)$$

It appears that the selected DFT functionals are not able to account for van der Waals dispersion forces, which are known to contribute substantially to the weak intermolecular interaction, for example, see refs 39−42. In the present study, the molecular crystals with moderate H-bonds[43] are considered. Their energy is larger than ~30 kJ/mol, and dispersion interactions are expected to play a minor role in the serine−H_2O and serine−H_2O_2 crystals. It was shown recently that the dispersion correction has little influence on the IR spectra.[44]

The CPMD calculations are done with the BLYP functional using Trouillier−Martins pseudopotentials for core electrons.[45] The kinetic energy cutoff for the plane wave basis set is 80 Ry. This value of the kinetic energy cutoff gives reasonable results for molecular crystals containing hydrogen and first-row elements.[46] Further increase of the kinetic energy cutoff practically up to 110 Ry does not change the computed values of the O−O, O···O, and O···N distances and the values of the harmonic frequencies. The *k*-space sampling was limited to the Γ point. Criterion on the maximum energy gradient component controlling the optimization process was set to 1×10^{-5} hartree/bohr. Tolerance on energy controlling the self-consistent field convergence for geometry optimization was set to 1×10^{-6} hartree. The minimum-energy states of the structures have been confirmed by calculating the harmonic frequencies. Step length in the numerical calculation of harmonic frequencies equals 0.01 Å.

MD Simulations. In the Car−Parrinello molecular dynamics (MD) runs, a fictitious electron mass of 900 au and a time step of 5 au (~0.12 fs) are employed. *NVT* simulations are performed at T = 298 K. The equilibrium structure serves as a starting point. The trajectory length is 4.5 ps. The kinetic energy cutoff for the plane wave basis set is 80 Ry. The value of the thermostat frequency is 3500 cm^{-1}.[30] The dipole moment function is obtained by the Berry phase approach of Resta,[47] as implemented in CPMD.[30]

The IR spectrum is obtained from the Fourier transform of the autocorrelation function of the classical dipole moment **M**[48] using:

$$I(\omega) = \left(\frac{2\pi\omega}{\varepsilon_0 chn}\right) F(\omega) Re \int_0^\infty e^{i\omega t} \langle \mathbf{M}(t)\mathbf{M}(0)\rangle \, dt \quad (2)$$

dx.doi.org/10.1021/jp207899z |J. Phys. Chem. A 2011, 115, 13657–13663

Table 1. Values of the O···X Distances R(O···X) and Angles ∠O···H−X of the O···H−X Fragment, Where X = O and N, in the Serine−H_2O Crystal: Experiment versus BLYP/6-311G and BLYP/80 Ry Computations at 0 K[a]**

	R(O···X), Å (∠O···H−X, deg)			ν(XH),[c] cm^{-1}	
H-bonded fragment[b]	exp[22]	BLYP/6-311G**	BLYP/80Ry	BLYP/6-311G**	BLYP/80Ry
O1···H3−N	2.890 (161)	2.8901 (168.9)	2.8602 (170.0)	3115 (1528), 3125 (2786), 3126 (95)	3032−3051
O1···H4−N	2.744 (149)	2.7314 (157.0)	2.7255 (156.9)	2995 (2487), 3110 (2842), 3113 (159)	2968−2973
O2···H7−O3	2.747 (167)	2.7461 (176.0)	2.7470 (175.3)	3201 (5081), 3214 (784), 3221 (499)	3232−3262
O2···Hw−1Ow	2.806 (169)	2.7832 (167.5)	2.7977 (165.2)	3455 (1971), 3460 (1542), 3466 (211)	3485−3499
O3···Hw2−Ow	2.836 (179)	2.7949 (175.0)	2.7983 (167.0)	3375 (1174), 3382 (1731), 3383 (795)	3426−3435
Ow···H2−N	2.879 (135)	2.8350 (141.4)	2.8060 (143.2)	3193 (493), 3195 (1972), 3205 (414)	3157−3171

[a] Computed values of the harmonic frequency of the H−X group stretching vibration are also given. [b] Numeration of amino acid atoms is introduced in Figure 1. [c] Computed values of the IR intensity (kM/mol) are given in parentheses.

Table 2. Values of the O···X Distances R(O···X) and Angles ∠O···H−X of the O···H−X Fragment, Where X = O and N, in the Serine−H_2O_2 Crystal: Experiment versus BLYP/6-311G and BLYP/80Ry Computations at 0 K[a]**

	R(O···X), Å (∠O···H−X, deg)			ν(XH),[c] cm^{-1}	
H-bonded fragment[b]	exp[52]	BLYP/6-311G**	BLYP/80Ry	BLYP/6-311G**	BLYP/80Ry
O1···H3−N	2.863 (171)	2.8888 (174.1)	2.8460 (176.3)	3012 (1841), 3024 (3200), 3025 (143)	2938−2943
O1···H4−N	2.779 (155)	2.8024 (154.3)	2.7791 (159.1)	3057 (1835), 3067 (2184), 3069 (62)	3022−3039
O2···H7−O3	2.731 (172)	2.6992 (172.6)	2.7051 (175.2)	3218 (5062), 3235 (1295), 3236 (562)	3216−3254
O2···H−Op2	2.716 (168)	2.7293 (161.1)	2.709 (164.7)	3332 (2593), 3340 (1708), 3345 (156)	3216−3254
O3···H−Op1	2.692 (162)	2.6440 (175.1)	2.6950 (161.2)	3170 (3678), 3173 (1042), 3192 (2518)	3261−3284
Op1···H2−N	2.833 (135)	2.7742 (139.2)	2.8123 (139.9)	3249 (218), 3250 (1499), 3257 (685)	3306−3364

[a] Computed values of the harmonic frequency of the H−X group stretching vibration are also given. [b] Selected H-bonds are introduced in Figure 2. [c] Computed values of the IR intensity (kM/mol) are given in parentheses.

where $I(\omega)$ is the relative IR absorption at frequency ω, c is the speed of light in vacuum, ε_0 is the dielectric constant of the vacuum, n is the refractive index, which is treated as constant, and $F(\omega)$ is a quantum correction factor. Different suggestions exist for the particular shape of $F(\omega)$.[49,50] The "harmonic" quantum correction factor seems to agree better with experimental data for molecular crystals with H-bonds, see, for example, Figure 2 in ref 51, and is therefore used for the spectra reported below.

RESULTS AND DISCUSSION

The Structure and Harmonic IR Spectrum. The unit cell parameters of the considered crystals obtained in the single-crystal X-ray studies[22,52] are adopted, and structural relaxations are limited to the positional parameters of atoms. The use of the experimental lattice parameters in the DFT computations of H-bonded crystals gives a reasonable description of the harmonic frequencies and IR intensities.[22,53,54] The experimental values of the atomic positions[22,52] are used as the starting point in the DFT computations with periodical boundary conditions. Optimization of the internal atomic coordinates started with the space groups established in the experimental studies. All of the structures are found to correspond to the stationary point on the potential energy surface.

In accord with the literature,[22,27] each serine molecule is involved in 10 H-bonds, six of which are unique, with both H_2O or H_2O_2 and neighboring serine molecules. The geometrical parameters of the six O···H−X fragments, X = O or N, and harmonic frequencies of the XH stretching vibrations obtained using the BLYP/6-311G** and BLYP/80Ry approximations are given in Tables 1 and 2. Computed values are in reasonable agreement with the experimental data. BLYP/6-311G** calculations predict ∼0.04 Å shorter O···O distance of the strongest O3···H-Op1 H-bond than the experimental value in the serine−H_2O_2 crystal, see Table 2 and Figures 1 and 2. A similar result was obtained in the DFT computations (PBE functional with dispersion correction) of the zwitterionic α-glycine crystal.[3] This drawback is absent in the BLYP/80Ry calculations.

Harmonic frequencies of the CH stretching vibrations of the title crystals are located in the 2900−3100 frequency region. Their IR intensities are negligible as compared to those of the NH and OH stretching vibrations. A similar result was obtained for the zwitterionic form of arginine solvated by a water molecule, see Figure 3 in ref 8. In accord with the experimental data, for example, see Table 1 in ref 55, the frequencies of the NH and OH vibrations are located above ∼2900 cm^{-1} (Tables 1 and 2), while the stretching vibrations of the CO_2 group and different bending vibrations lie below 1800 cm^{-1}. In harmonic approximation, the serine−H_2O and serine−H_2O_2 crystals have no fundamental vibrations in the ∼1800 to ∼2800 cm^{-1} frequency region. According to the experimental studies,[52] both crystals are characterized by IR-active bands in the ∼2500 to ∼2800 cm^{-1} region, see Figure 3. This discrepancy may be caused by the first overtone of the OH bending vibrations of H_2O and the combination vibration of the symmetric and asymmetric bendings of H_2O_2, for example, see refs 55,56. (Computed values of the OH bending vibrations of H_2O and H_2O_2 in the title crystals are located around 1440 cm^{-1}.) To verify this hypothesis, the

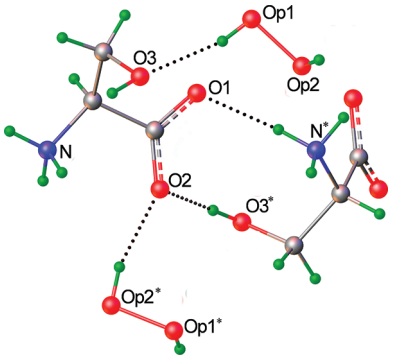

Figure 2. The fragment of the serine$-H_2O_2$ crystal. H-bonds are given by the broken lines. Asterisks denote the symmetry equivalent atoms.

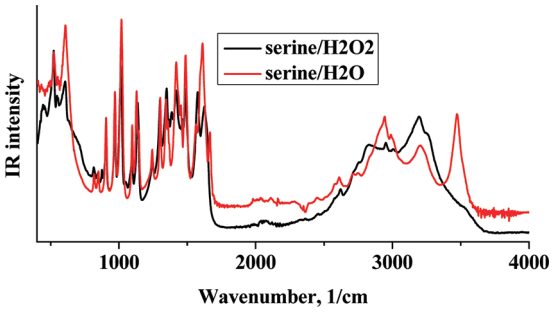

Figure 3. Experimental IR spectrum of the serine$-H_2O/H_2O_2$ crystals.

mid-IR spectra of the considered crystals were evaluated beyond the harmonic approximation.

Computed frequencies of the IR-active vibrations of the title crystals in the tetrahertz region are compared to the available experimental data in Table 3. The agreement is reasonable. Calculated values of the frequency shift of the serine$-H_2O$ crystal are systematically larger than the experimental ones. This may be caused by significant anharmonicity of lattice vibrations involving motions of cocrystallized H_2O molecules.[22] Tetrahertz frequencies of serine$-H_2O_2$ are located systematically lower than those of serine$-H_2O$. In contrast to serine$-H_2O$, serine$-H_2O_2$ has an IR-active band below 50 cm^{-1}, see Table 3. We can speculate that tetrahertz spectroscopy may be used to discriminate between the H_2O and H_2O_2 cocrystals of the given molecule (amino acid).

The H-Bond Network. Graph theory techniques were used in refs 57,58 to characterize the H-bond network in proton hydrates in the gas phase and in molecular crystals. In the present study, the Bader analysis[59] of the periodical electronic density is used for this purpose. It enables one to detect noncovalent interaction and H-bonds in the gas phase and periodical structures and to describe them quantitatively in terms of the Espinosa approach, for example, see refs 60,61. Computed values of electron density, ρ_b, at the O···H bond critical point are less than or equal to about 0.05 au (Tables 4 and 5). Taking into account that the respective values of the Laplacian of electron density, $\nabla^2\rho_b$, are positive, one comes to the conclusion that all intermolecular H-bonds in the considered crystals correspond to the shared interactions.[62,63] Energies of H-bonds in the title crystals, evaluated using eq 1, are given in Tables 4 and 5. In the serine$-H_2O$ crystal, the three unique H-bonds, forming by serine−serine

Table 3. Tetrahertz Vibrational Frequencies (ν, cm^{-1}) of the IR-Active Vibrations of Serine$-H_2O$ in the Range of 10−100 cm^{-1}: Experiment versus BLYP/6-311G Computations[a]**

serine$-H_2O$				serine$-H_2O_2$	
experiment[b]		BLYP/6-311G**		BLYP/6-311G**	
ν	$\Delta\nu$[c]	ν[d]	$\Delta\nu$	ν[d]	$\Delta\nu$
51.5[e]	−0.4	(57.7)[f]		48.4 (28.4)	−0.7
67.5	−0.8	66.2 (1.3)	−1.9	59.7 (8.4)	−1.6
75.7	−0.4	78.0 (9.1)	−3.7	69.9 (9.4)	−2.3
82.5	−0.5	88.8 (1.1)	−1.8	71.5 (19.0)	−2.4
88.1	−1.1	93.9 (27.2)	−3.7	85.3 (37.8)	−0.9
		96.8 (40.3)	−2.0	93.9 (0.8)	−2.2

[a] Computed frequencies of the serine$-H_2O_2$ crystal are also given. [b] See Table 2 in ref 22. [c] $\Delta\nu = \nu(d_6\text{-serine}-H_2O/H_2O_2) - \nu(\text{serine}-H_2O/H_2O_2)$, where d_6-serine$-H_2O/H_2O_2$ is deuterium-substituted serine$-H_2O/H_2O_2$. [d] Computed values of the IR intensity (kM/mol) are given in parentheses. [e] The small feature at 51.5 cm^{-1} appears in the 78 K spectrum as a result of the narrowing of the primary absorption band at 67.5 cm^{-1}.[22] [f] This band is IR-inactive in harmonic approximation.

interactions, are systematically stronger than the H-bonds between serine and H_2O. The O···H−N bonds in the considered hydrate are much stronger those in a serine crystal, cf., Tables 4 and 1 from ref 10. The energy of the weakest O···H−N interaction in serine$-H_2O$ (33 kJ/mol) is comparable to the energy of the strongest O···H−N bond in serine (27 kJ/mol). Each water molecule in serine$-H_2O$ is involved in three H-bonds. In two bonds, H_2O is the hydrogen donor, while in the third it is the hydrogen acceptor. The energy of the serine$-H_2O$ interactions varies from ∼29 to ∼37 kJ/mol and resembles the energy of the O···H−O bonds in serine, ∼37 kJ/mol.[10] According to our computations, H_2O is characterized by approximately equal hydrogen donor/acceptor properties in the serine$-H_2O$ crystal. The H_2O/H_2O_2 substitution does not change the H-bond network in the title crystals. The total energy of the three unique serine−serine H-bonds changes only negligibly (∼130 kJ/mol in serine$-H_2O$ vs ∼128 kJ/mol in serine$-H_2O_2$). On the other hand, the total energy of the serine$-H_2O_2$ bonds is ∼60 kJ/mol larger than those in serine$-H_2O$, in accord with experimental observations.[52] The main contribution to this value is the increase of the energy of the donor H-bonds formed by hydrogen peroxide in comparison with the energy of the corresponding bonds formed by H_2O. In other words, H_2O_2 is a better hydrogen donor than acceptor, at least in amino acid crystals.

Our computations led to the following series of H-bond strength in the crystals: serine < serine$-H_2O$ < serine$-H_2O_2$. In amino acid crystals, the H-bond network consists of amino acid−amino acid interactions. They are relatively weak, the energy of the O···H−N contacts not exceeding ∼35 kJ/mol. The H-bond network becomes much more complex in amino acid hydrates. The presence of water leads to an increase of the energy of the amino acid−amino acid interactions of up to ∼50 kJ/mol. The energy of the amino acid−water H-bonds is around 30 kJ/mol. The H_2O/H_2O_2 substitution does not change the H-bond network; however, the energy of the amino acid$-H_2O_2$ contacts may reach 60 kJ/mol. This is caused by the fact that H_2O_2 is a much better proton donor than H_2O in the title crystals.

Table 4. BLYP/6-311G Values of the O···H Distance, the Electron Density at the H-Bond Critical Point, ρ_b, and the Interaction Energy, E_{int}, of the Serine−H_2O Crystal**

interaction	H-bonded fragment	R(O···H), Å	ρ_b, au	E_{int}, kJ/mol
serine−serine	O1···H3−N	1.858	0.032	33.1
serine−serine	O1···H4−N	1.734	0.044	52.4
serine−serine	O2···H7−O3	1.748	0.041	46.8
serine−H_2O	O3···Hw1−Ow	1.807	0.033	36.5
serine−H_2O	O2···Hw2−Ow	1.814	0.031	35.3
serine−H_2O	Ow···H2−N	1.946	0.029	28.5

Table 5. BLYP/6-311G Values of the O···H Distance, the Electron Density at the H-Bond Critical Point, ρ_b, and the Interaction Energy, E_{int}, of the Serine−H_2O_2 Crystal**

interaction	H-bonded fragment	R(O···H), Å	ρ_b, au	E_{int}, kJ/mol
serine−serine	O1···H3−N	1.842	0.034	35.2
serine−serine	O1···H4−N	1.824	0.035	38.0
serine−serine	O2···H7−O3	1.705	0.045	54.3
serine−H_2O_2	O3···H−Op1	1.635[a]	0.052	68.0
serine−H_2O_2	O2···H−Op2	1.770	0.036	42.8
serine−H_2O_2	Op1···H2−N	1.903	0.030	31.2

[a] The O3···Op1 distance is shorter than the experimental value on 0.048 Å; see Table 2. This is why the value of electron density and energy of the O3···H contact may be overestimated.

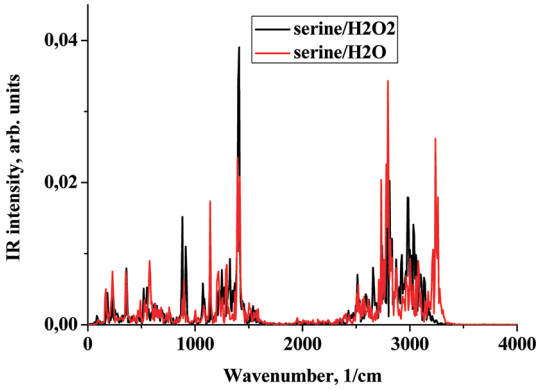

Figure 4. Computed anharmonic IR spectra of the serine−H_2O/H_2O_2 crystals.

Anharmonic Mid-IR Spectrum at 298 K. CPMD simulations are performed for the considered crystals to probe the potential (free) energy surface and to compute the anharmonic IR spectrum at temperature around the melting point of the crystals (298 K). According to our computations, all protons involved in the formation of H-bonds sit near the corresponding "heavy" atoms. The average O···(H)O and O···(H)N distances are larger that those at 0 K. This shows that proton-transfer phenomena are absent in the considered crystals. Computed anharmonic IR spectra of the crystals are given in Figure 4. In accord with the experimental observations, the IR spectra of both crystals are close to each other, cf., Figures 3 and 4. They differ in the high-frequency region only. The serine−H_2O crystal has an IR-intensive band around 3500 cm^{-1}, while there is only a shoulder in the experimental IR spectrum of serine−H_2O_2 (Figure 3). A similar result is obtained for the anharmonic IR spectra of the considered crystals (Figure 4). This difference supports the conclusion that the H-bonds in the serine perhydrate crystal are stronger than those in the serine hydrate crystal, cf., Tables 4 and 5.

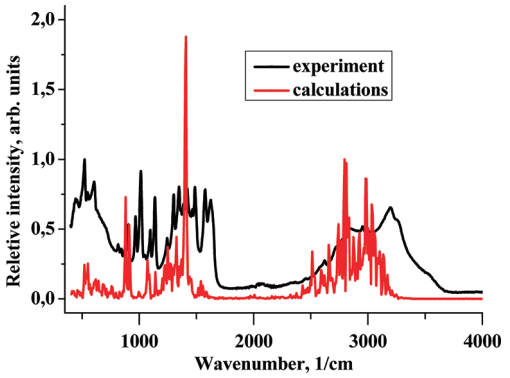

Figure 5. Experimental (black line) and computed anharmonic (red line) IR spectrum of the serine−H_2O_2 crystal.

Neither crystal has any IR-intensive bands in the 1700−2400 cm^{-1} frequency region. This situation is typical for the H-bonded crystals with the O···H−N^+ fragment, for example, see refs 21,64−66. On the other hand, IR-active bands appear around 2500 and 2750 cm^{-1} in the anharmonic spectra. They result from the first overtone of the OH bending vibrations of H_2O and the combined vibrations of the symmetric and asymmetric bendings of H_2O_2, respectively.

The computed anharmonic IR spectrum of the serine−H_2O_2 crystal agrees with the experimental one fairly well, see Figure 5. In the region above 3000 cm^{-1}, the bands in the theoretical spectrum shift to red in comparison with the experimental ones. We conclude that a reasonable description of the mid-IR spectrum of the amino acid perhydrate crystals is impossible in harmonic approximation.

CONCLUSIONS

The experimental IR spectrum of the serine−H_2O crystal in the low-frequency region is described fairly well in harmonic approximation. Computed frequencies of the IR-active vibrations of the titled crystals are quite different in the range of 10−100 cm^{-1}. In contrast to serine−H_2O, serine−H_2O_2 has an IR-active band below 50 cm^{-1}.

There are no fundamental bands in the 1800−2800 frequency region of both crystals in harmonic approximation. The IR-intensive bands in the 2500−2800 frequency region in the experimental IR spectra of the title crystals are caused by the first overtone of the OH bending vibrations of H_2O and the combined vibrations of the symmetric and asymmetric bendings of H_2O_2. These bands do exist in the computed anharmonic spectra.

The H-bond network in serine−H_2O is much more complex than that in serine. The presence of water leads to an increase of the energy of the amino acid−amino acid interactions, up to ∼50 kJ/mol. The energy of the amino acid−water H-bonds is around 30 kJ/mol. The H_2O/H_2O_2 substitution does not change the H-bond network, although the energy of the amino acid−H_2O_2 contacts increases up to 60 kJ/mol. This is caused by the fact that H_2O_2 is a much better proton donor than H_2O in the title crystals.

■ ASSOCIATED CONTENT

Supporting Information. Computed values of the O···X distances (Å) and angles (deg) of the O···H−X fragment, where X = O and N, in the serine−H_2O/H_2O_2 crystals: experiment versus DFT computations with periodic boundary conditions using the B3LYP and BLYP density functionals and Gaussian basis sets. This material is available free of charge via the Internet at http://pubs.acs.org.

■ AUTHOR INFORMATION

Corresponding Author
*E-mail: mikhail.vener@gmail.com.

■ ACKNOWLEDGMENT

We thank the Russian Foundation for Basic Research (grants 09-03-92476, 11-03-00583, 11-03-00551, and 11-03-92478), the Council on Grants of the President of the Russian Federation (NSh-8503.2010.3), and the Ministry of Education and Science of the Russian Federation (Federal Target program "Scientific and Pedagogical Staff of Innovating Russia 2009−2013", State Contract No. 16.740.11.0428). We acknowledge financial support from the infrastructure research program of the Israel Ministry of Science and the Israel National Fund. M.V.V. thanks Dr. V. A. Tikhomirov for useful comments.

■ REFERENCES

(1) Michalarias, I.; Beta, I. A.; Li, J. C.; Ruffle, S.; Ford, R. *J. Mol. Liq.* **2002**, *101*, 19.
(2) Ruffle, S.; Michalarias, I.; Li, J.-C.; Ford, R. C. *J. Am. Chem. Soc.* **2002**, *124*, 565.
(3) Maté, B.; Rodriguez-Lazcano, Y.; Gálvez, Ó.; Tanarro, I.; Escribano, R. *Phys. Chem. Chem. Phys.* **2011**, *13*, 12268 and references therein.
(4) Schener, S. *Phys. Chem. Chem. Phys.* **2011**, *13*, 13860.
(5) Vener, M. V.; Egorova, A. N.; Fomin, D. P.; Tsirelson, V. G. *J. Phys. Org. Chem.* **2009**, *22*, 177.
(6) Kong, S.; Shenderovich, I. G.; Vener, M. V. *J. Phys. Chem. A* **2010**, *114*, 2393.
(7) Blom, M. N.; Compagnon, I.; Polfer, N. C.; von Helden, G.; Meijer, G.; Suhai, S.; Paizs, B.; Oomens, J. *J. Phys. Chem. A* **2007**, *111*, 7309.
(8) Im, S.; Jang, S. W.; Lee, S.; Lee, Y.; Kim, B. *J. Phys. Chem. A* **2008**, *112*, 9767.
(9) Sun, J.; Bousquet, D.; Forbert, H.; Marx, D. *J. Chem. Phys.* **2010**, *133*, 114508.
(10) Rozenberg, M.; Shoham, G.; Reva, I.; Fausto, R. *Phys. Chem. Chem. Phys.* **2005**, *7*, 2376.
(11) Jarmelo, S.; Reva, I.; Carey, P. R.; Fausto, R. *Vib. Spectrosc.* **2007**, *43*, 395.
(12) Kolesov, B. A.; Boldyreva, E. V. *J. Phys. Chem. B* **2007**, *111*, 14387.
(13) Kolesov, B. A.; Boldyreva, E. V. *J. Raman Spectrosc.* **2010**, *41*, 670.
(14) Trivella, A.; Gaillard, T.; Stote, R. H.; Hellwig, P. *J. Chem. Phys.* **2010**, *132*, 115105.
(15) Siegrist, K.; Bucher, C. R.; Mandelbaum, I.; Walker, A. R. H.; Balu, R.; Gregurick, S. K.; Plusquellic, D. F. *J. Am. Chem. Soc.* **2006**, *128*, 5764.
(16) King, M. D.; Hakey, P. M.; Korter, T. M. *J. Phys. Chem. A* **2010**, *114*, 2945.
(17) Williams, M. R. C.; True, A. B.; Izmaylov, A. F.; French, T. A.; Schroeck, K.; Schmuttenmaer, C. A. *Phys. Chem. Chem. Phys.* **2011**, *13*, 11719.
(18) Franz, M.; Fischer, B. M.; Walther, M., doi:10.1016/j.molstruc.2011.05.061.
(19) Bordallo, H. N.; Boldyreva, E. V.; Buchsteiner, A.; Koza, M. M.; Landsgesell, S. *J. Phys. Chem. B* **2008**, *112*, 8748.
(20) Facanha, P. F.; Jiao, X. S.; Freire, P. T. C.; Lima, J. A.; dos Santos, A. O.; Henry, P. F.; Yokaichiya, F.; Kremner, E.; Bordallo, H. N. *Phys. Chem. Chem. Phys.* **2011**, *13*, 6576.
(21) Chowdhry, B. Z.; Dines, T. J.; Jabeen, S.; Withnall, R. *J. Phys. Chem. A* **2008**, *112*, 10333.
(22) King, M. D.; Buchanan, W. D.; Korter, T. M. *J. Phys. Chem. A* **2010**, *114*, 9570.
(23) Zakharov, B. A.; Kolesov, B. A.; Boldyreva, E. V. *Phys. Chem. Chem. Phys.* **2011**, *13*, 13106.
(24) Bienert, G. P.; Schjoerring, J. K.; Jahn, T. P. *Biochim. Biophys. Acta* **2006**, *1758*, 994.
(25) Miller, E. W.; Tulyathan, O.; Isacoff, E. Y.; Chang, C. J. *Nat. Chem. Biol.* **2007**, *3*, 263.
(26) Encrenaz, T.; Greathouse, T. K.; Richter, M. J.; Bezard, B.; Fouchet, T.; Lefevre, F.; Montmessin, F.; Forget, F.; Lebonnois, S.; Atreya, S. K. *Icarus* **2008**, *195*, 547.
(27) Prikhodchenko, P. V.; Medvedev, A. G.; Tripol'skaya, T. A.; Churakov, A. V.; Wolanov, Y.; Howard, J. A. K.; Lev, O. *CrystEngComm* **2011**, *13*, 2399.
(28) Allen, F. H. *Acta Crystallogr., Sect. B* **2002**, *58*, 380.
(29) Dovesi, R.; Saunders, V. R.; Roetti, C.; Orlando, R.; Zicovich-Wilson, C. M.; Pascale, F.; Civalleri, B.; Doll, K.; Harrison, N. M.; Bush, I. J.; D'Arco, Ph.; Llunell, M. *Crystal06 User's Manual*; Universita di Torino: Torino, 2006.
(30) Hutter, J.; Parrinello, M.; Alavi, A.; Marx, D.; Tuckerman, M.; Andreoni, W.; Curioni, A.; Fois, E.; Röthlisberger, U.; Giannozzi, P.; Deutsch, T.; Sebastiani, D.; Laio, A.; VandeVondele, J.; Seitsonen, A.; Billeter, S. *CPMD, 3.11.1*; IBM Research Laboratory and MPI für Festkörperforschung: Stuttgart, 1995−2007.
(31) Pascale, F.; Zicovich-Wilson, C. M.; Gejo, F. L.; Civalleri, B.; Orlando, R.; Dovesi, R. *J. Comput. Chem.* **2004**, *25*, 888.
(32) Zicovich-Wilson, C. M.; Dovesi, R.; Saunders, V. R. *J. Chem. Phys.* **2001**, *115*, 9708.
(33) Saunders, V. R.; Dovesi, R.; Roetti, C.; Causa, M.; Harrison, N. M.; Orlando, R.; Zikovich-Wilson, C. M. *CRYSTAL 98 User's Manual*; Universita di Torino: Torino, 1998.
(34) Gatti, C. *TOPOND98 User's Manual*; CNR-CSRSRC: Milano, Italy, 1999.
(35) Churakov, A. V.; Prikhodchenko, P. V.; Lev, O.; Medvedev, A. G.; Tripol'skaya, T. A.; Vener, M. V. *J. Chem. Phys.* **2010**, *133*, 164506.
(36) Vener, M. V.; Egorova, A. N.; Tsirelson, V. G. *Chem. Phys. Lett.* **2010**, *500*, 272.
(37) Espinosa, E.; Molins, E.; Lecomte, C. *Chem. Phys. Lett.* **1998**, *285*, 170.
(38) Sobczyk, L.; Grabowski, S. J.; Krygowski, T. M. *Chem. Rev.* **2005**, *105*, 3513 and references therein.
(39) Feng, S.; Li, T. *J. Chem. Theory Comput.* **2006**, *2*, 149.
(40) Civalleri, B.; Zicovich-Wilson, C. M.; Valenzano, L.; Ugliengo, P. *CrystEngComm* **2008**, *10*, 405.
(41) King, M. D.; Buchanan, W. D.; Korter, T. M. *Phys. Chem. Chem. Phys.* **2011**, *13*, 4250.
(42) Fedorov, I. A.; Zhuravleva, Y. N.; Berveno, V. P. *Phys. Chem. Chem. Phys.* **2011**, *13*, 5679.
(43) Steiner, T. *Angew. Chem., Int. Ed.* **2002**, *41*, 48.
(44) Akin-Ojo, A.; Wang, F. *Chem. Phys. Lett.* **2011**, *513*, 59.
(45) Troullier, N.; Martins, J. L. *Phys. Rev. B* **1991**, *43*, 1993.
(46) Tosoni, S.; Tuma, C.; Sauer, J.; Civalleri, B.; Ugliengo, P. *J. Chem. Phys.* **2007**, *127*, 154102.
(47) Resta, R. *Phys. Rev. Lett.* **1998**, *80*, 1800.
(48) Bosma, W. B.; Fried, L. E.; Mukamel, S. *J. Chem. Phys.* **1993**, *98*, 4413.
(49) Gaigeot, M.-P.; Sprik, M. *J. Phys. Chem. B* **2003**, *107*, 10344.
(50) Ramirez, R.; Lopez-Ciudad, T.; Kumar, P.; Marx, D. *J. Chem. Phys.* **2004**, *121*, 3973.

(51) Vener, M. V.; Sauer, J. *Phys. Chem. Chem. Phys.* **2005**, *7*, 258.
(52) Churakov, A. V.; Prikhodchenko, P. V.; Howard, J. A. K.; Lev, O. *Chem. Commun.* **2009**, 4224.
(53) Zicovich-Wilson, C. M.; San-Roman, M. L.; Camblor, M. A.; Pascale, F.; Durand-Niconoff, J. S. *J. Am. Chem. Soc.* **2007**, *129*, 11512.
(54) Vener, M. V.; Manaev, A. V.; Tsirelson, V. G. *J. Phys. Chem. A* **2008**, *112*, 13628.
(55) Arnau, J. L.; Giguere, P. A.; Abe, M.; Taylor, R. C. *Spectrochim. Acta* **1974**, *30A*, 777.
(56) Pettersson, M.; Tuominen, S.; Räsänen, M. *J. Phys. Chem.* **1997**, *101*, 1166.
(57) Jieli, M.; Aida, M. *J. Phys. Chem. A* **2009**, *113*, 1586.
(58) Hayes, R. L.; Paddison, S. J.; Tuckerman, M. E. *J. Phys. Chem. B* **2009**, *113*, 16574.
(59) Bader, R. F. W. *Atoms in Molecules. A Quantum Theory*; Oxford University Press: New York, 1990.
(60) Vener, M. V.; Egorova, A. N.; Fomin, D. P.; Tsirelson, V. G. *Chem. Phys. Lett.* **2007**, *440*, 279.
(61) Vener, M. V.; Egorova, A. N.; Fomin, D. P.; Tsirelson, V. G. *J. Mol. Struct.* **2010**, *972*, 11.
(62) Gatti, C. *Z. Kristallogr.* **2005**, *220*, 399.
(63) Vener, M. V.; Manaev, A. V.; Egorova, A. N.; Tsirelson, V. G. *J. Phys. Chem. A* **2007**, *111*, 1155.
(64) Majerz, I.; Sawka-Dobrowolska, W.; Sobczyk, L. *J. Mol. Struct.* **1993**, *297*, 177.
(65) Majewska, P.; Pajak, M.; Rospenk, M.; Filarowski, A. *J. Phys. Org. Chem.* **2009**, *22*, 130.
(66) Jezierska-Mazzarello, A.; Panek, J. J.; Vuilleumier, R.; Koll, A.; Ciccotti, G. *J. Chem. Phys.* **2011**, *134*, 034308.